

See discussions, stats, and author profiles for this publication at: <https://www.researchgate.net/publication/222127154>

Mojave Mars simulant—Characterization of a new geologic Mars analog

Article in Icarus · October 2008

DOI: 10.1016/j.icarus.2008.05.004

CITATIONS

39

READS

278

8 authors, including:



Greg Peters

NASA

26 PUBLICATIONS 82 CITATIONS

[SEE PROFILE](#)



Greg Bearman

ANE Image

142 PUBLICATIONS 1,708 CITATIONS

[SEE PROFILE](#)



Greg S. Mungas

Hyperlight Energy

126 PUBLICATIONS 163 CITATIONS

[SEE PROFILE](#)

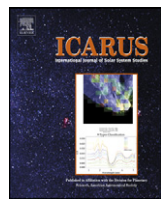
Some of the authors of this publication are also working on these related projects:



Low Cost Concentrated Solar Power [View project](#)



Mars 2020: SHERLOC [View project](#)



Mojave Mars simulant—Characterization of a new geologic Mars analog

Gregory H. Peters^a, William Abbey^b, Gregory H. Bearman^a, Gregory S. Mungas^a, J. Anthony Smith^a, Robert C. Anderson^b, Susanne Douglas^b, Luther W. Beegle^{b,*}

^a *In Situ Instrument Systems Section, Jet Propulsion Laboratory, California Institute of Technology, 4800 Oak Grove Drive, Pasadena, CA 91109-8099, USA*

^b *Planetary Science Section, Jet Propulsion Laboratory, California Institute of Technology, 4800 Oak Grove Drive, Pasadena, CA 91109-8099, USA*

ARTICLE INFO

Article history:

Received 4 March 2007

Revised 1 May 2008

Available online 27 May 2008

Keywords:

Mars, surface

Geological processes

Experimental techniques

Regoliths

ABSTRACT

We have identified and characterized a basaltic Mars simulant that is available as whole rocks, sand and dust. The source rock for the simulant is a basalt mined from the Tertiary Tropico Group in the western Mojave Desert. The Mojave Mars Simulant (MMS) was chosen for its inert hygroscopic characteristics, its availability in a variety of forms, and its physical and chemical characteristics. The MMS dust and MMS sand are produced by mechanically crushing basaltic boulders. This is a process that more closely resembles the weathering/communition processes on Mars where impact events and aerodynamic interactions provide comminution in the (relative) absence of water and organics. MMS is among the suite of test rocks and soils that was used in the development of the 2007/8 Phoenix Scout and is being used in the 2009 Mars Science Laboratory (MSL) missions. The MMS development team is using the simulant for research that centers on sampling tool interactions in icy soils. Herein we describe the physical properties and chemical composition of this new Mars simulant.

© 2008 Elsevier Inc. All rights reserved.

1. Introduction

In order to better design and test the next generation of Mars missions, a regolith simulant that adequately represents the various dust, soil and rock properties that exist on the martian surface is required. As one recent MEPAG (Mars Exploration Program Analysis Group) report specifically states, an important strategy for reducing the risks related to the effects of granular materials on both engineering and biological systems on Mars is to establish one or more martian dust/regolith simulants, then make them available in bulk quantities for the development and testing of sample acquisition/processing hardware, as well as scientific instruments, here on Earth (Beatty et al., 2005).

The Mars simulant currently in common use is JSC Mars-1 (Allen et al., 1998). JSC Mars-1 is a glassy, meteorically altered volcanic ash from Pu'u Nene, a late Pleistocene cinder cone located on the flanks of Mauna Kea, Hawaii (Allen et al., 1998). This material is basaltic in nature and has long been recognized as a good spectral analog for the bright regions on Mars (Evans and Adams, 1979; Singer, 1982; Morris et al., 1993). In 1997, researchers from the Johnson Space Center excavated a 40–60 cm thick zone of this unconsolidated material and then dried and sieved it to separate out the <1 mm size fraction. This size fraction has been made available to researchers for the past decade as JSC Mars-1 and has

seen widespread use throughout the scientific community (examples include Lepper and McKeever, 2000; Carpenter et al., 2003; Ormond and Kral, 2006).

When JSC-Mars-1 was developed, the knowledge of the physical characteristics of the martian surface was limited primarily to orbital/remote observations and those made by the Viking landers. At both Viking landing sites (VL-1 and VL-2), the regolith was classified as a fine-grained, cohesionless to rocky soil that contained small duricrust clods and possible rock fragments (Banin et al., 1992). Over the past decade three additional landing sites have been examined demonstrating a range of martian surface characteristics. At the Mars Pathfinder site, regolith can best be described as a combination of thin drifts of bright red, fine-grained material, soil-like deposits and rocks (Moore et al., 1999). In contrast, the Mars Exploration Rover (MER) Spirit found that the floor of Gusev Crater is dominated by basaltic sand grains and lithic fragments that have been disrupted by impact events and modified by eolian processes (Greeley et al., 2004; Herkenhoff et al., 2004a; Squyres et al., 2004a). At the same time MER Opportunity discovered that surface material throughout Meridiani Planum is dominated by sand-sized basaltic grains (<125 μm), sulfate-rich outcrop debris, and hematite-rich spherules and fragments (Herkenhoff et al., 2004b; Soderblom et al., 2004; Squyres et al., 2004b). All of these locations also contain variable amounts of fine-grained atmospheric dust. For other regions, where landed missions have yet to investigate, including ones where recent observations indicate the presence of sulfate and phyllosilicate minerals, there is likely a good deal of regolith and dust mixing from impacts and planet-wide dust storms

* Corresponding author. Fax: +1 818 393 4445.

E-mail address: luther.beegle@jpl.nasa.gov (L.W. Beegle).

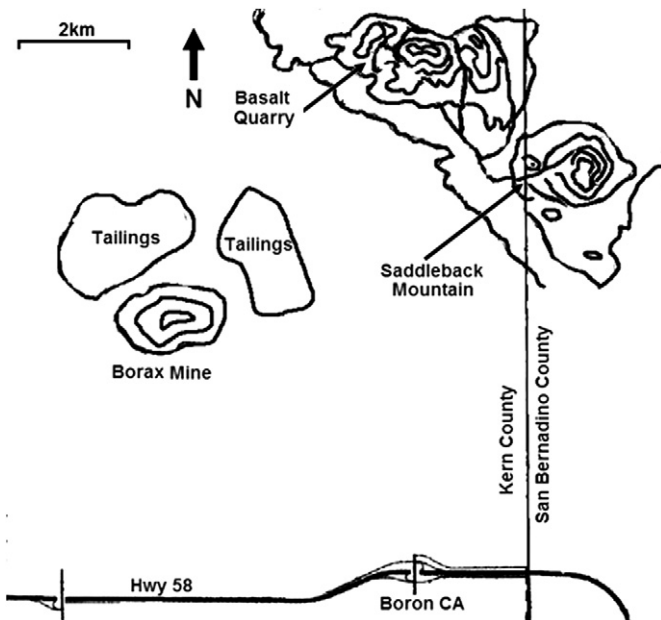


Fig. 1. Graphical representation of the Saddleback basalt formation in the western Mojave Desert of eastern California (long. -117.62507 , lat. 35.05751).

([Banin et al., 1992](#); [Bibring et al., 2006a, 2006b](#)). The bulk component can be reasonably simulated for basaltic regions of Mars using the MMS as a feedstock. Identifying the bulk component allows the end user to make modifications to satisfy particular chemical, mineralogical and physical components for testing of engineering requirements and performing scientific experiments.

We should point out at this time that it was not our original intention to develop another martian simulant. However, while performing a series of experiments to measure water sublimation loss on excavated permafrost under ambient martian conditions ([Peters et al., 2008](#)), we discovered that the hygroscopic tendency of JSC Mars-1 made it difficult to reproduce our results. Simply put, dried JSC Mars-1 gained moisture too quickly for our purposes. While the actual hygroscopicity of martian regolith is unknown at this time, it was advantageous for our particular research to use a material that would gain ambient moisture mass at a much slower rate. Our search for less hygroscopic, less weathered material eventually led us to the Saddleback Basalt in the Mojave Desert which was subsequently used to develop the Mojave Mars Simulant (MMS) here at the Jet Propulsion Lab (JPL). Characterizing this new simulant is the subject of this paper.

1.1. Saddleback Basalt

The source rock for the MMS is the Saddleback Basalt ([Fig. 1](#)), which consists of one or more basalt flows, about 100 m in total thickness, interbedded with sediments comprising the middle portion of the Tertiary Tropico Group near Boron, California, in the western Mojave Desert ([Dibblee, 1958, 1967](#)). These flows outcrop discontinuously from Saddleback Mountain, just north of Boron, northwestward for ~ 12 km and westward for ~ 25 km. It is worth noting that the source location for the MMS is only a few kilometers away from one of the largest borate mines in the world. In fact the basalts stratigraphically underlie the famous borate-bearing shales of the Kramer mining district ([Siefke, 1991](#)). In hand sample, the Saddleback Basalt is dark gray to black, massive, aphanitic or very fine-grained to finely ophitic in texture and contains scattered phenocrysts of fine-grained plagioclase feldspar. In the field it weathers reddish brown with exposed surfaces locally displaying a dark brown varnish. Abundant vesicles also are locally com-

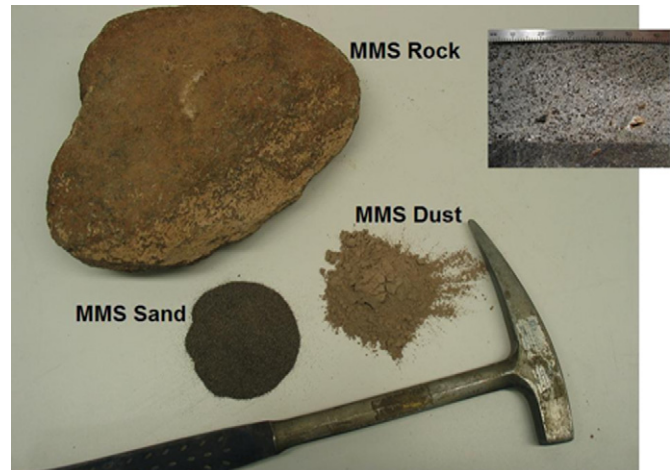


Fig. 2. Image of the MMS whole rock, sand and dust. The inset is cut face of MMS whole rock. The bottom edge of the inset shows an unweathered/broken (as opposed to saw-cut) surface.

mon. The Saddleback Basalt is early Miocene in age and has been radiometrically dated to 20 Ma ([Armstrong and Higgins, 1973](#); [Golombek and Brown, 1988](#)). However, it is interesting to note that it seems to be genetically and chemically unrelated to other Miocene volcanics in the immediate area ([Putirka and Weigand, 1987](#)).

2. Samples and methods

2.1. Collection site

During initial field reconnaissance we were fortunate to discover that the Saddleback Basalt is currently being mined by Carlton Global Resources. This operation, located near Saddleback Mountain, excavates the basalt as whole rock and then proceeds to crush and screen this material on-site. The main commercial products of this operation are granular chips and sand, both of which are used in the manufacture of asphalt shingles. At the time of this writing, the granular product is only available in bulk to Carlton's primary customer, so it was not considered for characterization. The sand, however, is available in large quantities to outside consumers (like ourselves). Also available in large quantities are unprocessed whole rock and fine basaltic dust, a by-product of the rock crushing process. During crushing, the airborne dust is collected via a large vacuum system to comply with air quality regulations. All three available products have found use as MMS source material here at JPL, and we have concentrated our efforts on characterizing all these types, namely the whole rock, sand and dust ([Fig. 2](#)).

2.2. Samples

In order to ensure that the chemical composition and mineralogy of these products are consistent as Carlton excavates progressively deeper layers of basalt, we collected two sets of sand and dust samples from the mine nearly one year apart, in the fall of 2006 (MMS sand and dust I) and the summer of 2007 (MMS sand and dust II). We also gathered hand samples of the whole rock from various locations throughout the formation.

2.3. Analytical methods

Physical properties of the MMS whole rock were determined by the Newmont Rock Mechanics Laboratory at the Mining Engineering Department of the Colorado School of Mines. They determined

uniaxial compressive strength, static elastic constants, dynamic elastic constants, tensile strength (Brazilian Index), abrasivity (Cerchar index) and hardness (Schmidt hammer). Concentrations of both major and trace elements for whole rock samples were determined by ALS Chemex during the initial development of the mining operation (2005–06). Major elements were obtained using inductively coupled plasma atomic emission spectroscopy (ICP-AES). Trace elements were obtained using both ICP-AES and ICP-MS (mass spectroscopy) following digestion of the basalt in nitric-perchloric-hydrofluoric acid and leaching of the resulting cake in hydrochloric acid.

Earth Systems Engineering Inc. conducted physical properties tests on the MMS sand, dust and JSC Mars-1. A “Standard Test Method for Particle-Size Analysis” (ASTM D-422) was used to quantitatively determine the distribution of particle sizes in the samples. The distribution of particle sizes larger than 75 µm was determined by sieving, while the size distribution of smaller particles was determined by a sedimentation process, using a hydrometer to secure the necessary data. Also, a “Standard Test Method for Direct Shear” (ASTM D-3080) was used to determine the consolidated drained shear strength of the samples under direct shear. This test was performed by deforming three or more specimens, each under a different normal load, at a controlled strain rate on or near a single shear plane. The volatile content was determined by heating ~10 g of both sand and dust to 100 and 500 °C for 1 h each in a bench top Blue M, Lab Heat Muffle Furnace and immediately measuring the mass loss of the sample. For the sake of comparison, these tests were also conducted on JSC Mars-1.

The MMS whole rock, sand and dust were further characterized using additional instruments available at JPL. Samples were examined using a FEI (Philips) XL 30 environmental scanning electron microscope (ESEM) equipped with a field emission electron gun. An accelerating voltage of 20 keV with a beam current of 264 µA was used for backscatter imaging and to excite X-ray emission from the samples. Elemental analysis was performed using an EDAX Genesis energy dispersive X-ray spectrometer (EDS) with an ultrathin window, allowing detection of elements down to and including boron. A Bruker AXS model D8 Discover X-ray diffractometer equipped with a General Area Detector Diffraction System (GADDS) using CuK α radiation ($\lambda = 0.1542$ nm) was employed to obtain powder XRD patterns for the samples. In order to determine if smectites and/or other phyllosilicates are present oriented samples of clay-size fractions (<4 µm; obtained by gravity sedimentation of an aqueous dispersion), with and without ethylene glycol solvation, were prepared and analyzed according to the methods outlined by Moore and Reynolds (1997). Peak identifications were made based on standard powder diffraction files from the International Centre for Diffraction Data (ICDD), 2000. We obtained reflectance spectra for all of the MMS materials using an ASD Inc. FieldSpec3 spectroradiometer with a solar simulation light source. This instrument combines three spectrometers in a single instrument to measure a wide range of the solar spectrum (350–2500 nm).

3. Characterization

3.1. Mineralogy

XRD patterns for the MMS are dominated by peaks associated with plagioclase feldspar and Ca-rich pyroxene as well as minor magnetite. Trace amounts of ilmenite (Fe, Ti oxide) and Fe-rich olivine also are suggested by XRD as well as by ESEM-EDS data (Fig. 3). These results are consistent with the original observations of Saddleback Mountain and classify the MMS as an olivine basalt (Dibblee, 1967; Garrett, 1998). In addition, all MMS samples have

XRD peaks corresponding to varying amounts of hematite, consistent with the reddish brown weathering product observed in hand sample. ESEM-EDS analysis further suggests that a Mn oxide (perhaps manganite) is also present in or on some samples which may be attributed to the desert varnish that coats many of these rocks. Local amygdalites, vesicular cavities filled with a secondary, mineral present throughout the basalt, primarily play host to carbonate and silica, however ESEM-EDS data also suggests the presence of Ba sulfate (possible barite), Ca phosphate (possible apatite) and much rarer minerals such as zeolites, also noted in the literature (Housley, 2004). This secondary mineralization most likely formed during one or more low temperature hydrothermal events, possibly in association with the deposition of nearby borate deposits. It should also be noted that no phyllosilicates or crystalline clay minerals were observed by either XRD or ESEM in the MMS.

By way of comparison, JSC Mars-1 is an altered volcanic ash (palagonitic tephra) composed of finely crystalline and glassy particles of hawaiitic composition (Morris et al., 1993; Allen et al., 1998). The fine crystals are primarily plagioclase feldspar and minor Ti magnetite, but Ca-rich pyroxene and olivine are also present. The majority of iron (~64%) occurs as nanophase (<20 nm) ferric oxide particles. But it should be noted that JSC Mars-1 contains less than 1 wt% of crystalline clay minerals or phyllosilicates. The most significant difference between the two simulants is that MMS is largely crystalline, while JSC Mars-1 is primarily glassy in texture.

On Mars, the surface is dominated by dark basaltic sand composed primarily of pyroxene and plagioclase feldspar with minor amounts of olivine and various Fe, Ti oxides, probably magnetite and/or hematite (Goetz et al., 2005; Yen et al., 2005; Morris et al., 2006a, 2006b). This material is most likely derived from the physical weathering of a variety of intermediate to basic igneous rocks ranging from the olivine basalts discovered at Gusev Crater by the Spirit Rover (Christensen et al., 2004a; Morris et al., 2006a) to the andesitic “soil free rock” derived from Pathfinder data (Wanke et al., 2001; Foley et al., 2003). The composition of this sand is further modified by sulfate and hematite contamination and, possibly, the presence of minor carbonates (Scott et al., 1997; Borg et al., 1999). This contamination seems to vary a great deal locally but is particularly abundant at Meridiani Planum which features both sulfate-rich outcrops and hematite spherules (“blueberries”) (Christensen et al., 2004b; Morris et al., 2006b). All of these features tend to be obscured to one degree or another by the ubiquitous, global dust that imparts the surface of Mars with its characteristic red-orange color. Up to one third of this dust is likely composed of nanophase ferric oxide particles (Klingelhofer et al., 2004).

The MMS suite is similar to and provides a good mineralogic analog for the igneous rocks of Mars and their associated weathering products. Plagioclase feldspar and pyroxene, along with minor olivine and magnetite, tend to be the dominant minerals in both the MMS and the martian rocks. As one might guess, differences can primarily be found in the composition of individual mineral phases. For example, plagioclase tends to be sodic to intermediate in composition at Gusev Crater while MMS plagioclase tends to be more calcic in composition (Christensen et al., 2004a). Also, while most data for martian rocks tends to favor the presence of Ca-rich pyroxene, subordinate amounts of Ca-poor pyroxene has also been suggested in some places (Foley et al., 2003; Christensen et al., 2004a, 2004b). In contrast, JSC Mars-1 more closely resembles the global dust as both are composed of nanophase ferric oxide particles and fine-grained basaltic minerals and glass. It should be noted that neither simulant is a good mineralogical match with regards to any sulfate or carbonate contamination.

Table 1

Chemical composition of MMS whole rock samples. Total iron expressed as Fe₂O₃. Loss on ignition (LOI) measured at 1000 °C, includes H₂O, SO₃ and Cl. Major element abundances, expressed as oxides, are in weight percent (wt%). Trace element abundances are in ppm (μg/g), except where noted, and are listed by increasing atomic number. It should be noted that REEs (*in italics*) may not be totally soluble in four-acid digestion technique described in methods

| MMS whole rocks | | | | | | | | | | |
|------------------------------------|--------|--------|--------|--------|--------|--------|--------|--------|--------|--------|
| #1 | #2 | #3 | #4 | #5 | #6 | #7 | #8 | #9 | #9a | |
| <i>Concentration in wt%</i> | | | | | | | | | | |
| SiO ₂ | 47.7 | 47.8 | 49.7 | 47.2 | 47.6 | 47.7 | 47.5 | 48.2 | 47.1 | 47.1 |
| TiO ₂ | 0.89 | 1.10 | 0.95 | 1.24 | 1.14 | 0.95 | 1.19 | 1.20 | 0.87 | 0.93 |
| Al ₂ O ₃ | 16.5 | 16.7 | 16.8 | 16.8 | 16.1 | 17.4 | 16.4 | 17.1 | 15.5 | 16.1 |
| Cr ₂ O ₃ | 0.04 | 0.06 | 0.04 | 0.06 | 0.06 | 0.05 | 0.06 | 0.06 | 0.04 | 0.05 |
| Fe ₂ O ₃ T | 10.80 | 10.70 | 10.65 | 10.60 | 9.84 | 11.30 | 10.35 | 10.75 | 9.73 | 10.25 |
| MnO | 0.19 | 0.17 | 0.17 | 0.18 | 0.16 | 0.17 | 0.17 | 0.16 | 0.15 | 0.14 |
| MgO | 6.45 | 7.17 | 4.68 | 5.72 | 6.49 | 6.13 | 4.83 | 5.40 | 6.09 | 5.93 |
| CaO | 10.30 | 10.60 | 9.66 | 11.45 | 10.50 | 10.20 | 10.25 | 10.25 | 7.85 | 8.60 |
| Na ₂ O | 2.51 | 3.39 | 3.19 | 3.55 | 3.44 | 3.34 | 4.11 | 2.95 | 2.12 | 2.34 |
| K ₂ O | 0.42 | 0.47 | 0.50 | 0.43 | 0.39 | 0.56 | 0.58 | 0.33 | 0.47 | 0.41 |
| P ₂ O ₅ | 0.15 | 0.23 | 0.20 | 0.20 | 0.25 | 0.16 | 0.11 | 0.11 | 0.10 | 0.09 |
| LOI | 2.83 | 1.24 | 2.20 | 2.29 | 1.69 | 2.05 | 5.27 | 3.13 | 9.79 | 7.77 |
| Total | 98.8 | 99.6 | 98.7 | 99.7 | 97.6 | 100 | 100 | 99.6 | 99.8 | 99.7 |
| <i>Concentration in ppm (μg/g)</i> | | | | | | | | | | |
| Li | 19.0 | 17.8 | 16.3 | 16.9 | 15.9 | 15.6 | 15.0 | 18.6 | 55.1 | 49.0 |
| S (in wt%) | 0.09 | 0.07 | 0.12 | 0.03 | 0.03 | 0.03 | <0.01 | <0.01 | <0.01 | <0.01 |
| V | 179 | 201 | 166 | 197 | 198 | 136 | 205 | 220 | 124 | 158 |
| Co | 49.1 | 44.8 | 47.0 | 43.7 | 42.3 | 44.4 | 39.7 | 44.1 | 39.3 | 41.6 |
| Ni | 113.0 | 66.4 | 118.0 | 38.0 | 42.3 | 107.5 | 33.9 | 40.5 | 88.2 | 89.2 |
| Cu | 64.2 | 55.3 | 61.0 | 49.6 | 49.7 | 54.0 | 50.3 | 69.1 | 65.6 | 57.7 |
| Zn | 73 | 75 | 71 | 75 | 76 | 64 | 67 | 82 | 65 | 74 |
| Ga | 16.3 | 17.6 | 17.3 | 18.1 | 17.8 | 16.7 | 17.4 | 20.1 | 15.3 | 17.8 |
| Ge | 0.07 | 0.07 | 0.07 | 0.07 | 0.06 | 0.07 | 0.06 | 0.15 | 0.13 | 0.14 |
| As | 70.3 | 34.4 | 2.7 | 12.9 | 8.0 | 2.9 | 51.0 | 27.5 | 46.8 | 45.5 |
| Se | <1 | <1 | <1 | <1 | <1 | <1 | <1 | 2 | 2 | 2 |
| Rb | 11.9 | 9.3 | 13.0 | 9.9 | 8.9 | 7.4 | 14.8 | 6.5 | 15.4 | 15.4 |
| Sr | 278 | 341 | 263 | 341 | 315 | 219 | 287 | 296 | 213 | 265 |
| Y | 23.9 | 24.6 | 25.1 | 24.1 | 23.0 | 20.9 | 23.7 | 26.1 | 19.4 | 23.3 |
| Zr | 88.8 | 100.5 | 100.0 | 109.0 | 104.0 | 61.2 | 101.5 | 113.5 | 74.6 | 89.4 |
| Nb | 4.0 | 4.5 | 5.4 | 4.3 | 4.3 | 4.0 | 4.2 | 4.5 | 3.2 | 3.2 |
| Mo | 0.79 | 0.54 | 0.89 | 0.64 | 0.58 | 0.29 | 0.67 | 0.81 | 0.43 | 0.48 |
| Ag | 0.05 | 0.04 | 0.05 | 0.04 | 0.05 | 0.03 | 0.03 | 0.04 | 0.03 | 0.04 |
| Cd | 0.11 | 0.11 | 0.08 | 0.14 | 0.11 | 0.05 | 0.05 | 0.05 | 0.02 | 0.04 |
| In | 0.055 | 0.056 | 0.055 | 0.059 | 0.054 | 0.045 | 0.052 | 0.070 | 0.054 | 0.057 |
| Sn | 0.8 | 0.9 | 1.0 | 0.9 | 0.8 | 0.8 | 0.8 | 1.0 | 0.7 | 0.8 |
| Sb | 3.22 | 0.92 | 0.40 | 0.32 | 0.22 | 0.67 | 2.13 | 0.67 | 0.79 | 0.93 |
| Te | <0.05 | <0.05 | <0.05 | <0.05 | <0.05 | <0.05 | <0.05 | <0.05 | <0.05 | <0.05 |
| Cs | 0.68 | 0.49 | 0.73 | 0.41 | 0.33 | 0.36 | 0.74 | 0.51 | 1.38 | 1.37 |
| Ba | 630 | 2040 | 290 | 560 | 360 | 200 | 160 | 180 | 150 | 180 |
| La | 8.8 | 10.5 | 9.8 | 8.8 | 8.9 | 6.6 | 7.8 | 8.0 | 6.0 | 7.0 |
| Ce | 21.6 | 21.3 | 22.9 | 21.6 | 19.9 | 16.2 | 18.5 | 19.0 | 13.6 | 15.7 |
| Hf | 2.4 | 2.8 | 2.7 | 2.8 | 2.8 | 1.8 | 2.8 | 2.9 | 2.0 | 2.3 |
| Ta | 0.29 | 0.31 | 0.39 | 0.29 | 0.29 | 0.29 | 0.28 | 0.31 | 0.24 | 0.27 |
| W | 0.5 | 0.3 | 0.4 | 0.2 | 0.1 | 0.4 | 0.4 | 0.4 | 0.7 | 0.7 |
| Re | <0.002 | <0.002 | <0.002 | <0.002 | <0.002 | <0.002 | <0.002 | <0.002 | <0.002 | <0.002 |
| Tl | 0.10 | 0.05 | 0.06 | 0.07 | 0.05 | 0.05 | 0.10 | 0.07 | 0.06 | 0.07 |
| Pb | 4.6 | 3.1 | 4.5 | 3.6 | 2.6 | 3.7 | 2.5 | 2.1 | 2.0 | 2.3 |
| Bi | 0.02 | 0.02 | 0.01 | 0.01 | 0.01 | 0.01 | <0.01 | 0.02 | 0.01 | 0.01 |
| Th | 1.8 | 1.5 | 2.2 | 1.3 | 1.2 | 1.5 | 1.1 | 1.3 | 1.3 | 1.5 |

3.2. Chemistry

Table 1 shows the chemical composition of nine MMS whole rock samples selected from a variety of locations on or near Saddleback Mountain. It is important to note that samples #6 and #7 were collected from subvolcanic intrusive layers of the basalt and that sample #9a is the 3/8–9/16 inch (~5–7.5 mm) particle size fraction of sample #9 after being crushed and screened. It is also important to note that none of these samples vary significantly from the bulk of the MMS which is remarkably uniform in geochemical composition. The only major difference between samples can be seen in the trace element abundances of Ba and As, but this local variation is most likely related to secondary fluids and appears to have little influence on the chemistry of major elements.

Table 2 compares the chemical composition of both the MMS simulant and the JSC Mars-1 simulant to the martian regolith de-

scribed at the Viking, Pathfinder, and MER landing sites. The bulk of this material can be described as “soil” but it should be noted that this term is used here only to distinguish loose, unconsolidated material from rocks and bedrock and that no implication as to the presence or absence of organic matter is intended. In addition to soil data, the composition of select rocks described at these sites has also been included in this table. For Pathfinder, the “soil free rock” or SFR was calculated by Foley et al. (2003) using a linear regression technique as outlined by Wanke et al. (2001) to subtract the composition of surface dust from that of the underlying rocks. For data from the Spirit Rover this subtraction is unnecessary as the rocks we chose to include (Adirondack, Humphrey and Mazatzal) had their compositions determined after surface dust was removed by the rock abrasion tool (RAT) (Gellert et al., 2004). This is also the case for Bounce, the single rock measured by Opportunity included in Table 2 (Rieder et al., 2004).

Table 2

Chemical composition of martian regolith compared to the composition of martian simulants. All data (except VL-1 and VL-2) has been normalized with the assumption that samples are free of water and carbonates and that S is present as SO_3 . No attempt was made to normalize Viking data as contributions from various sources of uncertainty are not well constrained (Clark, 1993); in addition to potential volatile loss, there are issues of grain size heterogeneity and the inability to detect certain elements (Na, P, Mn) due to interference from major peaks (Mg, Cl, Fe). For the Viking Landers, Pathfinder "soil", JSC Mars-1 and MMS total iron is expressed as Fe_2O_3 ; for Pathfinder SFR, MER Spirit and MER Opportunity total iron is expressed as FeO . Loss on ignition (LOI) for JSC Mars-1 was measured at 950 °C, includes H_2O , SO_3 and Cl. All elemental abundances are in weight percent (wt%).

| Martian regolith | | | | | | | | Martian simulants | |
|--------------------------------|-------|------------------|------|--|------------------------|-----------------|--------|-------------------|----------------------------------|
| Viking Landers | | Pathfinder | | MER Spirit | | MER Opportunity | | JSC Mars-1 | MMS |
| VL-1 | VL-2 | "Soil" | SFR | "Soil" | Rocks | "Soil" | Bounce | | |
| <i>Concentration in wt%</i> | | | | | | | | | |
| SiO ₂ | 43 | 43 | 42.0 | 57.7 | 45.8 | 45.6 | 43.8 | 50.8 | 43.48 |
| TiO ₂ | 0.66 | 0.56 | 0.8 | 0.50 | 0.81 | 0.55 | 1.08 | 0.78 | 3.62 |
| Al ₂ O ₃ | 7.3 | (7) ^a | 10.3 | 12.3 | 10.0 | 10.6 | 8.6 | 10.1 | 22.09 |
| Cr ₂ O ₃ | – | – | 0.3 | – | 0.35 | 0.56 | 0.46 | 0.12 | 0.03 |
| Fe ₂ O ₃ | 18.5 | 17.8 | 21.7 | – | – | – | – | – | 16.08 |
| FeO | – | – | 14.2 | 15.8 | 17.8 | 22.3 | 15.6 | – | 10.87 |
| MnO | – | – | 0.3 | 0.5 | 0.31 | 0.38 | 0.36 | 0.43 | 0.26 |
| MgO | 6 | (6) ^a | 7.3 | 0.8 | 9.3 | 10.7 | 7.1 | 6.4 | 4.22 |
| CaO | 5.9 | 5.7 | 6.1 | 6.7 | 6.10 | 7.50 | 6.67 | 12.5 | 6.05 |
| Na ₂ O | – | – | 2.8 | 4.2 | 3.3 | 3.0 | 1.6 | 1.3 | 2.34 |
| K ₂ O | <0.15 | <0.15 | 0.6 | 1.2 | 0.41 | 0.15 | 0.44 | 0.10 | 0.70 |
| P ₂ O ₅ | – | – | 0.7 | 0.4 | 0.84 | 0.67 | 0.83 | 0.95 | 0.78 |
| SO ₃ | 6.6 | 8.1 | 6.0 | 0.25 | 5.82 | 1.79 | 5.57 | 0.52 | 0.31 ^b |
| Cl | 0.7 | 0.5 | 0.9 | 0.4 | 0.53 | 0.23 | 0.44 | 0.06 | – |
| LOI | – | – | – | – | – | – | – | – | (17.36) |
| Total | 89 | 89 | 99.8 | 99.2 | 99.4 | 99.6 | 99.3 | 99.7 | 99.7 |
| Mean of Method Source | 3 | 3 | 7 | 5 | 11 | 3 | 8 | 1 | 2 ^b |
| X-ray fluorescence | | | | Alpha Particle X-ray Spectrometer (APXS) | | | | | XRF |
| (Banin et al., 1992) | | | | (Foley et al., 2003) | (Gellert et al., 2004) | | | | ICP-AES (Morris et al., 2000) |

“–” not analyzed.

^a Al₂O₃ and MgO not measured by VL-2 due to instrument difficulties; values assumed to be same as for VL-1.

^b SO₃ for JSC Mars-1 determined from a single unheated sample using a sulfur analyzer.

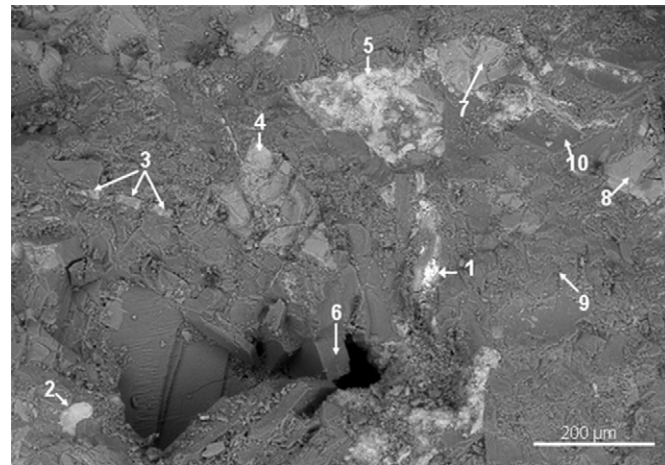


Fig. 3. A typical ESEM image of the MMS whole rock generated via backscatter imaging. Contrast is derived from differences in atomic mass, heavier elements appear as brighter areas (ex. point 1, which is rich in barium) and lighter elements give a darker signal (ex. point 10, which is rich in boron). Elemental abundances can be found in Table 3.

It should be mentioned that the emphasis here was on igneous rocks and that non-igneous rocks, such as the sulfur-rich sediments found at Meridiani Planum, were not considered for this comparison.

As seen in Table 2 the martian soil is globally homogenized with a geochemical composition that remains extremely consistent between landing sites. The only major variation seems to occur in the abundance of Fe and is most likely due to the presence (or lack thereof) of weathering debris from local iron-rich sources such as the hematite spherules at Meridiani Planum (Rieder et al., 2004). Compared to the martian soil the MMS has higher levels of SiO₂, Al₂O₃ and CaO and lower levels of total Fe and P₂O₅, while JSC

Table 3

Elemental abundances for each analysis point as seen in Fig. 3. These values were obtained by EDS and are given in weight percent (wt%). Error varies from ± 7.0 wt% for B to ± 0.05 wt% for Mn, to which the spectrometer is calibrated. Suggested mineralogy for noted points are: 1 = Ba sulfate; 2 = Fe oxide; 3 = Fe, Ti oxide; 4 and 8 = Fe-rich olivine; 5 = Mn oxide; 6 and 9 = groundmass (basalt); 10 = high-B silicate

| EDS analysis | | | | | | | | | | |
|--------------------------|------|------|------|------|------|------|------|------|------|------|
| 1 | 2 | 3 | 4 | 5 | 6 | 7 | 8 | 9 | 10 | |
| <i>Abundances in wt%</i> | | | | | | | | | | |
| B | 0.0 | 0.0 | 0.0 | 0.0 | 0.0 | 0.0 | 0.0 | 11.7 | 0.0 | 12.7 |
| Na | 1.5 | 1.5 | 1.8 | 1.2 | 1.4 | 3.0 | 1.5 | 1.3 | 2.9 | 4.1 |
| Mg | 3.4 | 2.6 | 1.9 | 8.8 | 2.6 | 1.1 | 7.0 | 7.8 | 0.9 | 0.8 |
| Al | 6.0 | 4.4 | 5.3 | 2.8 | 3.4 | 13.0 | 4.2 | 2.6 | 13.1 | 8.0 |
| Si | 18.8 | 13.4 | 14.4 | 15.8 | 6.9 | 20.9 | 17.3 | 14.0 | 20.5 | 21.0 |
| S | 2.5 | 0.0 | 0.0 | 0.0 | 0.0 | 0.0 | 0.0 | 0.0 | 0.0 | 0.0 |
| K | 0.2 | 0.3 | 0.6 | 0.2 | 1.1 | 0.0 | 0.2 | 0.1 | 0.0 | 1.9 |
| Ca | 2.6 | 1.8 | 2.9 | 1.0 | 1.3 | 5.8 | 1.7 | 1.0 | 5.8 | 1.4 |
| Ti | 0.0 | 0.0 | 19.4 | 0.0 | 0.0 | 0.0 | 0.0 | 0.0 | 0.0 | 0.0 |
| Ba | 15.8 | 0.0 | 0.0 | 0.0 | 2.4 | 0.0 | 0.0 | 0.0 | 0.0 | 0.0 |
| Mn | 0.7 | 0.0 | 0.0 | 0.6 | 24.9 | 0.5 | 1.6 | 0.8 | 0.1 | 0.9 |
| Fe | 14.9 | 29.4 | 12.2 | 18.2 | 1.1 | 1.3 | 24.3 | 15.0 | 0.9 | 1.1 |
| Oxygen | 33.6 | 46.6 | 41.5 | 51.4 | 54.9 | 54.4 | 42.2 | 45.7 | 55.8 | 48.1 |

Mars-1 has higher levels of TiO₂ and Al₂O₃ and lower levels of MgO. In addition, all martian soils are characterized by elevated concentrations of SO₃ and Cl, evidence of extensive mixing with evaporites and possible salt formation (Haskin et al., 2005). MMS and JSC Mars-1 both lack this distinctive characteristic.

The igneous rocks studied on Mars exhibit a great deal more variation than the soil. They include geochemically primitive (low SiO₂ and K₂O and high MgO) picritic basalts at Gusev Crater (McSween et al., 2004) more geochemically evolved (higher SiO₂ and K₂O and lower MgO) basaltic andesites at the Pathfinder landing site and Bounce Rock at Meridiani Planum which has an intermediate basaltic character consistent with shergottites (martian meteorites of basaltic composition) (Rieder et al., 2004). Geochem-

ically, the MMS is most similar to Bounce although the MMS is much higher in Al_2O_3 and significantly lower in total Fe. However, this is not surprising as martian rocks are characteristically high in Fe and low in Al, this is believed to reflect the original composition of the martian mantle (Gellert et al., 2004). JSC Mars-1 is most similar to the basalts of Gusev Crater except JSC Mars-1 is higher in TiO_2 and Al_2O_3 and lower in CaO and K₂O. It is worth noting that these trends may be exaggerated as the source rock for JSC Mars-1 has experienced extensive palagonization which can cause in situ leaching of both Si and alkalis and cause enrichment in Ti, Al, and total Fe (Morris et al., 1993; Carpenter et al., 2003).

3.3. Physical properties

Table 4 collects the physical properties of the unconsolidated MMS simulants and JSC Mars-1. As can be seen in this table the angle of friction of both the MMS sand (38°) and dust (31°) are comparable to the martian values as observed at the Pathfinder, VL-1 and VL-2 sites and are significantly less than those of JSC Mars-1 (Moore and Jakosky, 1989; Moore et al., 1999). In addition, the density of both the MMS sand and dust compare closer to that observed on Mars and are significantly denser than JSC Mars-1. Tables 5 and 6 present the physical properties of three different MMS whole rock as collected.

Table 4

Physical properties of the MMS sand and dust components compared to JSC Mars-1 and material found at different martian landing sites

| | Angle of friction | Cohesion (kPa) | Dry density (kg/m^3) |
|-----------------------------------|----------------------------|-----------------|---------------------------------|
| MMS sand I | 38° | 0.81 | 1384 |
| MMS sand II | 39° | 1.96 | 1341 |
| MMS dust I | 31° | 0.38 | 1078 |
| MMS dust II | 30° | 0.53 | 911 |
| JSC Mars-1 | 47° | 1.91 | 835 |
| Pathfinder | | | |
| Drift material ^a | 34.3° | 0.21 | 1285 to 1518 |
| Crusty material ^a | $37.0^\circ \pm 2.6^\circ$ | 0.17 ± 0.18 | 1422 to 1636 |
| Viking Landers | | | |
| VL-1 drift material ^b | $18.0^\circ \pm 2.4^\circ$ | 1.6 ± 1.2 | 1150 ± 150 |
| VL-1 blocky material ^b | $30.8^\circ \pm 2.4^\circ$ | 5.1 ± 2.7 | 1600 ± 400 |
| VL-2 crusty material ^b | $34.5^\circ \pm 4.7^\circ$ | 1.1 ± 0.8 | 1400 ± 200 |

^a Mars Pathfinder physical property results were derived from rover imagery and observed soil/rover wheel interactions. In general, soil properties can vary significantly depending on the nature of the deposit (i.e. eolian deposit, surface deposit with cementation, layering, and varying particle size distribution). More description of the experimental technique for deriving soil properties can be found in Moore et al. (1999).

^b Moore and Jakosky (1989).

Table 5

Strength properties of the MMS whole rocks

| | Uniaxial compressive strength (MPa) | Brazilian tensile strength (MPa) | Cerchar abrasivity index | Schmidt hardness index |
|------------|-------------------------------------|----------------------------------|--------------------------|------------------------|
| MMS Rock-1 | 144 | 7.2 | 4.9 | 42.9 |
| MMS Rock-2 | 118 | 6.9 | 5.1 | 37.8 |
| MMS Rock-3 | 89 | 7.9 | 5.1 | 37.8 |

Table 6

Elastic constants of the MMS whole rocks

| | Static elastic constants | | P-wave velocity (m/s) | S-wave velocity (m/s) | Dynamic elastic constants | |
|------------|--------------------------|-----------------|-----------------------|-----------------------|---------------------------|-----------------|
| | Young's modulus (GPa) | Poisson's ratio | | | Young's modulus (GPa) | Poisson's ratio |
| MMS Rock 1 | 59 | 0.24 | 5224.27 | 2917.24 | 59 | 0.27 |
| MMS Rock 2 | Not analyzed | Not analyzed | 5085.89 | 2762.71 | 51 | 0.29 |
| MMS Rock 3 | Not analyzed | Not analyzed | 5003.90 | 2786.79 | 52 | 0.28 |

3.4. Reflectance spectra

Reflectance patterns varied with particle size distribution and we found that the MMS sand is closely matched with JSC Mars-1, as shown in Fig. 4a. The agreement between MMS, and JSC-1 and the composite reference spectra for Mars are all similar (Mustard and Bell, 1994). Each has a rise in the reflectance value from 400–700 nm, with an absorption band in the 770–930 nm region and a generally flat reflectance from 1000–2400 μm as shown in Fig. 4a. Figs. 4b–4d are the average reflectance spectra, from Telescopic, IRS (Mariner 6 and 7) and ISM (Phobos-2), spectra of two regions, one light (Ophir Planum) and one dark (Eos Chasma) (Erard and Calvin, 1997). While the region between 1000–2500 nm is generally flatter in the remote observations, when compared to the sand, dust and JSC-1 spectra in that range, this could be an artifact of viewing geometries. The reflectance spectra obtained at the Pathfinder landing site, Figs. 4c–4d, all possess the same general trend as both the MMS sand, MMS dust and JSC-Mars-1, with the main difference being the lack of a well-defined absorption feature in the JSC Mars-1. The spectra obtained at the MER landing sites show the

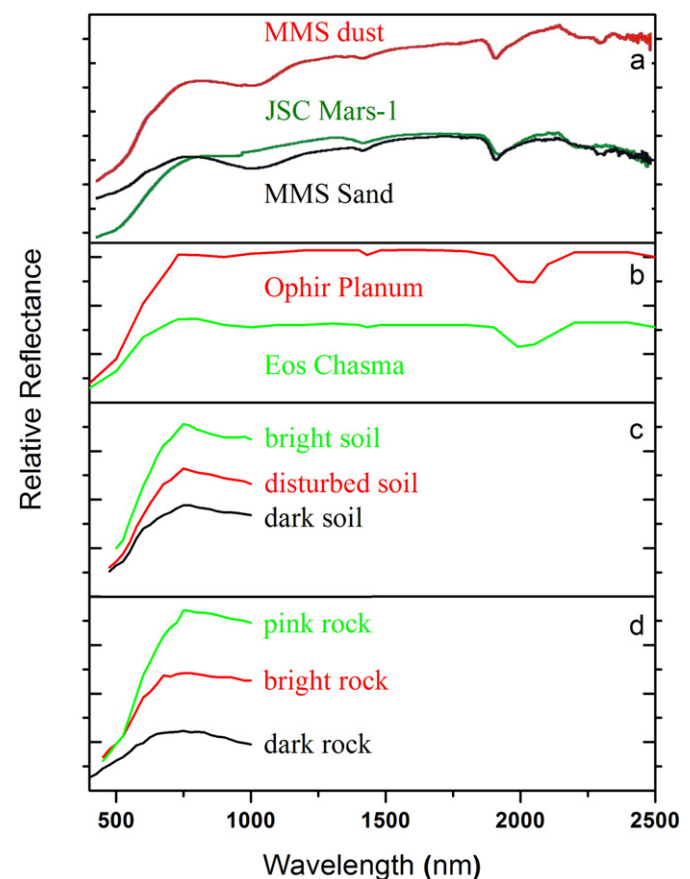


Fig. 4. UV-Vis-NIR reflectance spectra of MMS dust, sand and JSC Mars-1 (a) compared to orbital observations (b), as well as soil (c) and rock types (d) observed at the Pathfinder landing site (Erard and Calvin, 1997; Smith et al., 1997a). The description of the nomenclature for features from the Pathfinder data can be found in Smith et al. (1997a).

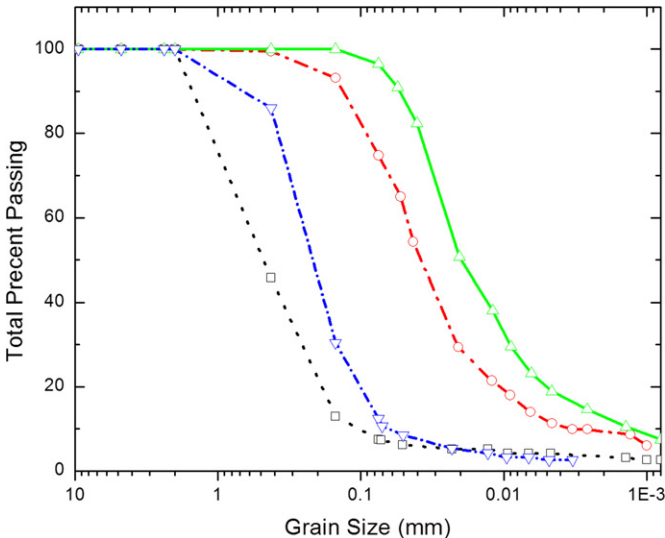


Fig. 5. MMS component particle size distributions of MMS dust I and II (triangles and circles, respectively), MMS sand (upside down triangles), and JSC Mars-1 (squares) (ASTM D422).

same general trends as the Pathfinder data and are consistent with the MMS spectra (Bell et al., 2004a, 2004b).

3.5. Volatile content and hygroscopicity

The volatile loss of the MMS dust was ~ 1.7 wt% at 100°C , 7.2 wt% at 500°C , which most likely is dominated by H_2O . In contrast, it is estimated that the martian soils analyzed by Viking released on the order of $0.1\text{--}1.0$ wt% when they were heated to 500°C , consisting mostly of water, and JSC Mars-1 loses 21.1 wt% when heated to 600°C (Allen et al., 1998).

While the exact hygroscopic nature of martian soil is unknown, by absorbing water the physical properties of a material can change. This can be a serious problem for experiments and testing that occur over many months and/or experience wide variations in climatic conditions. For example, we placed 10 g of desiccated material on a Denver instruments microbalance during a relatively humid day (78% relative humidity). During a 5-min period JSC Mars-1 gained ~ 0.1 wt% every 5 min while MMS dust gained <0.01 wt% over the same 5-min interval.

3.6. Magnetic properties

The martian regolith has a 1–7 wt% magnetic component according to data gathered at the Viking, and Pathfinder landing sites while the magnetic component determined at Gusev was ~ 2 wt% (Smith et al., 1997b; Madsen et al., 1999, 2003; Bertelsen et al., 2004). A hand magnet was used to gather the magnetic material from ten samples of the MMS dust and it was determined to have an average magnetic component of ~ 5 wt% versus ~ 25 wt% for JSC Mars-1 (Allen et al., 1998). The magnetic minerals in MMS are most likely ilmenite (Fe, Ti oxide) and hematite as suggested by the XRD and ESEM-EDS data, while the magnetic component on the surface of Mars is comprised mainly of magnetite (Goetz et al., 2005; Morris et al., 2006b). However, it should be noted that both ilmenite and hematite have also been identified as constituents in martian surface material (McSween et al., 2004; Morris et al., 2006b).

3.7. Size distribution

Fig. 5 shows the measured particle size distribution for MMS dust I, dust II, MMS sand I and JSC Mars-1. The dust has a consid-

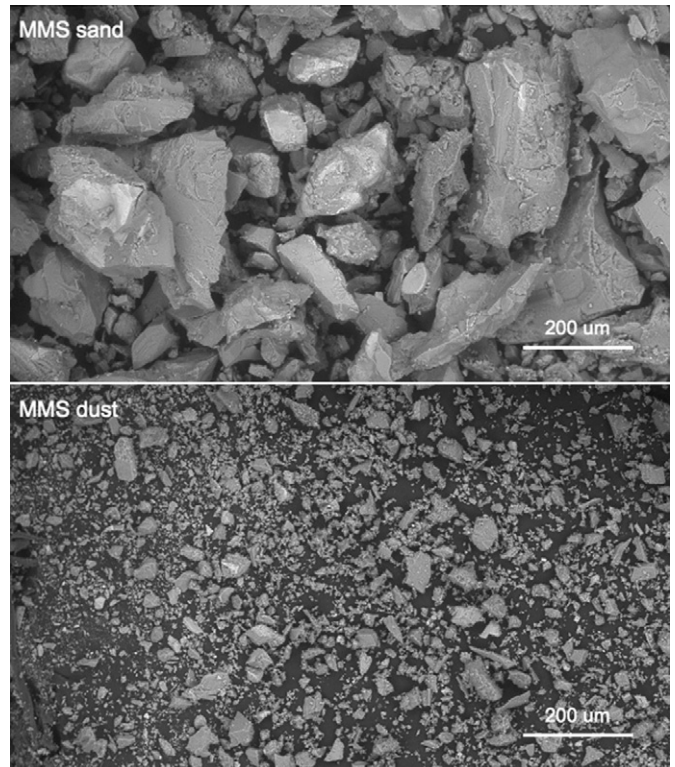


Fig. 6. ESEM images of MMS sand and dust generated via backscatter imaging. Contrast is derived from differences in atomic mass, heavier elements appear as brighter areas and tend to correspond to Fe, Ti oxides, while lighter elements give a darker signal and tend to correspond to the basaltic groundmass and local carbonates.

erably larger fraction of smaller particles than either the sand or JSC Mars-1 which both show a grain fraction of ~ 5 wt% for sizes 5–52 μm and a grain fraction of less than 1 wt% for sizes $< 5 \mu\text{m}$. Martian surface material predominantly consists of particles that are less than 50 μm in size as inferred from observations made during the Viking, Pathfinder and MER missions. Images from the Viking landing sites were used to determine that the average size for “drift material” ranges from 0.1–10 μm , while more “blocky material” ranges up to 1.5 mm in grain size (Ballou et al., 1978; Christensen and Moore, 1992). All four landers also noted the ubiquitous dust that is suspended in the martian atmosphere. The grain size of these dust particles was determined by atmospheric observations to be on the order of 1–2 μm (Pollack et al., 1979; Smith and Lemmon, 1999; Clancy et al., 2003; Lemmon et al., 2004).

Fig. 6 is an ESEM image showing that both the MMS dust and sand occur as angular shards, almost conchoidal in fracture habit. It should also be noted here that XRD data of the $< 5 \mu\text{m}$ size fraction, as well as extensive observations made under the ESEM, suggests that there is no preferential mineral fractionation based on grain size in the MMS. This is important to note, as a “normal” grain size distribution for rocks that have been diminished by natural weathering processes tends to skew in favor of Fe oxides and clay minerals at the finest grain sizes and it is rare to find an abundance of feldspar in the less than 10–20 μm size fraction (Moore and Reynolds, 1997). The lack of these trends in the MMS samples is most likely an artifact of the crushing process.

4. Conclusions

On Earth, soils are created through various weathering processes that have most commonly involve water and/or biochemical interactions. However, on Mars and planetary environments that

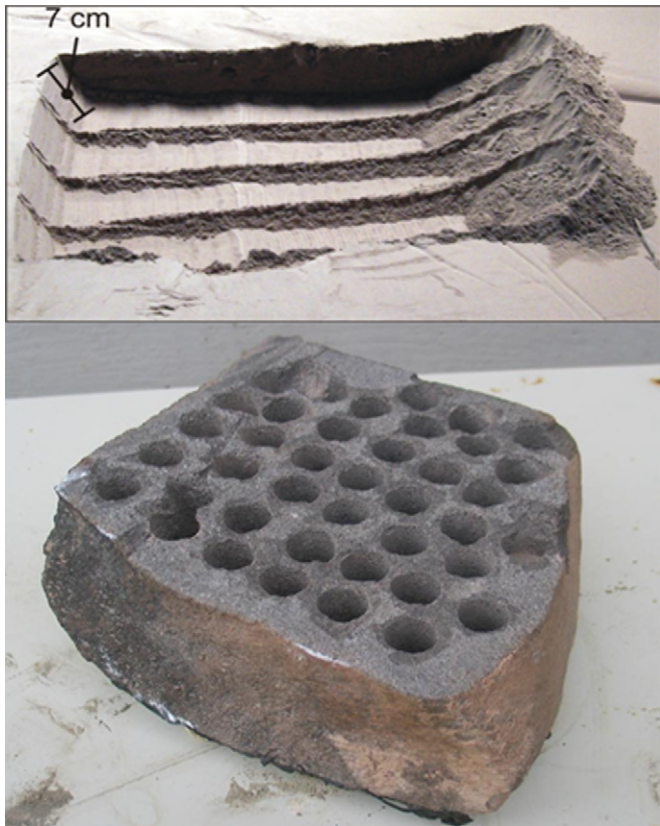


Fig. 7. Trench dug into dust during Phoenix robotic arm and scoop testing and an MMS rock with holes made using a Mars sampling drill under development.

are and were likely devoid of the levels of liquid water and biochemistry that exists on Earth, these weathering processes will be, to first order, dominated by physical weathering involving mechanical comminution processes. Even though secondary minerals unveil the fingerprints of terrestrial weathering, the MMS rocks are nearly pristine by Earth standards. Given enough time, the MMS rocks will eventually decompose into what will be unquestionably, terrestrial soil. However our (geologic) timing is good (give or take a few million years) and the MMS sand and the MMS dust may be produced by mechanically crushing whole rocks in the (relative) absence of water and organics. These new soils have undergone a process that more closely resembles the weathering/comminution processes on Mars and planetary environments where impact events and aerodynamic interactions (in the case of Mars) with geologic soils provide mechanical mechanisms for comminution.

The basaltic rock found at the Saddleback Mountain is currently being used for the testing of future Mars mission platforms, the development of future instruments, and to help us better understand the physical nature of the martian near surface. It has been used to test the robotic scoop and rapid active sample package (RASP) on the Phoenix Scout lander as well as the drill, the mobility and landing systems on the 2009 Mars Science Laboratory (MSL) rover (Fig. 7). MMS has also been used as a simulant soil for the testing of yearly hydrological cycles in high latitudes and, most recently, it was employed in an extensive experimental program to measure the volatile loss from analog martian permafrost samples during sampling with the RASP, currently on the Phoenix mission (Peters et al., 2008).

In order to simulate martian regolith more accurately, we propose that the MMS be used as a bulk base material and then spiked with additives, such as carbonate, sulfate or other evaporate mineral. This would augment the chemical nature of the MMS

basalt thus creating more realistic simulants of the martian surface. We currently are storing ~10 tons of both the MMS dust and sand, and plan on obtaining more material as space permits. In addition at every eventual run, a new series of tests will be performed to characterize the new batch to demonstrate uniform mineral, physical and chemical properties.

Acknowledgments

This research was carried out at the Extraterrestrial Material Simulation Laboratory at the Jet Propulsion Laboratory, California Institute of Technology, and was supported under internal RT&D funding. We wish to acknowledge David Oliver of Select Resources for the initial tour of the basalt mining facilities and for providing the geochemical data; Brandon Griffiths of US Borax for arranging a tour of the borax mine and providing information regarding the local stratigraphy; Marshal Petit of Carlton Global Resources for allowing access to the crushing and screening facilities and for providing both samples and processing information; and Tim Thomson of Earth Systems Engineering for performing the direct shear and particle size distribution tests. We would also like to thank Dr. Pamela Conrad of JPL for graciously allowing us access to her Bruker X-ray diffractometer. Finally we greatly appreciate the comments from two anonymous reviewers for immeasurably improving this paper.

References

- Allen, C.C., Jager, K.M., Morris, R.V., Lindstrom, D.J., Lindstrom, M.M., Lockwood, J.P., 1998. JSC Mars-1: A Martian Soil Simulant. *Space* 98, San Diego, CA.
- Armstrong, R.L., Higgins, R.E., 1973. K-Ar dating of beginning of tertiary volcanism in Mojave Desert, California. *Geol. Soc. Am. Bull.* 84 (3), 1095–1099.
- Ballou, E.V., Wood, P.C., Wydeven, T., Lehwalt, M.E., Mack, R.E., 1978. Chemical interpretation of Viking Lander 1 life detection experiment. *Nature* 271 (5646), 644–645.
- Banin, A., Clark, B.C., Wanke, H., 1992. Surface chemistry and mineralogy. In: Kieffer, H.H., Jakosky, B.M., Snyder, C.W., Matthews, M.S. (Eds.), *Mars*. The University of Arizona Press, Tucson, pp. 594–625.
- Beatty, D.W., Snook, K., Allen, C.C., Eppler, D., Farrell, W.M., Heldmann, J., Metzger, P., Peach, L., Wagner, S.A., Zeitlin, C., 2005. An analysis of the precursor measurements of Mars needed to reduce the risk of the first human missions to Mars. Posted by the Mars Exploration Program Analysis Group (MEPAG), Pasadena, at <http://mepag.jpl.nasa.gov/reports/index.html>, June 2005.
- Bell, J.F., Squyres, S.W., Arvidson, R.E., Arneson, H.M., Bass, D., Blaney, D., Cabrol, N., Calvin, W., Farmer, J., Farrand, W.H., Goetz, W., Golombek, M., Grant, J.A., Greeley, R., Guinness, E., Hayes, A.G., Hubbard, M.Y.H., Herkenhoff, K.E., Johnson, M.J., Johnson, J.R., Joseph, J., Kinch, K.M., Lemmon, M.T., Li, R., Madsen, M.B., Maki, J.N., Malin, M., McCartney, E., McLennan, S., McSweeney, H.Y., Ming, D.W., Moersch, J.E., Morris, R.V., Dobrea, E.Z.N., Parker, T.J., Proton, J., Rice, J.W., Seelos, F., Soderblom, J., Soderblom, L.A., Sohl-Dickstein, J.N., Sullivan, R.J., Wolff, M.J., Wang, A., 2004a. Pancam multispectral imaging results from the Spirit Rover at Gusev Crater. *Science* 305 (5685), 800–806.
- Bell, J.F., Squyres, S.W., Arvidson, R.E., Arneson, H.M., Bass, D., Calvin, W., Farrand, W.H., Goetz, W., Gotombek, M., Greeley, R., Grotzinger, J., Guinness, E., Hayes, A.G., Hubbard, M.Y.H., Herkenhoff, K.E., Johnson, M.J., Johnson, J.R., Joseph, J., Kinch, K.M., Lemmon, M.T., Li, R., Madsen, M.B., Maki, J.N., Malin, M., McCartney, E., McLennan, S., McSweeney, H.Y., Ming, D.W., Morris, R.V., Dobrea, E.Z.N., Sullivan, R.J., Weitz, C.M., Wolff, M.J., 2004b. Pancam multispectral imaging results from the Opportunity Rover at Meridiani Planum. *Science* 306 (5702), 1703–1709.
- Bertelsen, P., Goetz, W., Madsen, M.B., Kinch, K.M., Hviid, S.F., Knudsen, J.M., Gunnlaugsson, H.P., Merrison, J., Nornberg, P., Squyres, S.W., Bell, J.F., Herkenhoff, K.E., Gorevan, S., Yen, A.S., Myrick, T., Klingelhofer, G., Rieder, R., Gellert, R., 2004. Magnetic properties experiments on the Mars Exploration Rover Spirit at Gusev Crater. *Science* 305 (5685), 827–829.
- Bibring, J.P., Langevin, Y., Mustard, J.F., Poulet, F., Arvidson, R., Gendrin, A., Gondet, B., Mangold, N., Pinet, P., Forget, F., 2006a. Global mineralogical and aqueous Mars history derived from OMEGA/Mars Express data. *Science* 312 (5772), 400–404.
- Bibring, J.P., Squyres, S.W., Arvidson, R.E., 2006b. Merging views on Mars. *Science* 313 (5795), 1899–1901.
- Borg, L.E., Connelly, J.N., Nyquist, L.E., Shih, C.Y., Wiesmann, H., Reese, Y., 1999. The ages of the carbonates in martian meteorite ALH84001. *Science* 286 (5437), 90–94.

- Carpenter, P., Sebille, L., Boles, W., Chadwell, M., Schwarz, L., 2003. JSC Mars-1 martian soil simulant: Melting experiments and electron microprobe studies. *Microsc. Microanal.* 9, 30–31.
- Christensen, P.R., Moore, H.J., 1992. The martian surface layer. In: Kiefer, H.H., Jakosky, B.M., Snyder, C.W., Matthews, M.S. (Eds.), *Mars*. University of Arizona Press, Tucson, pp. 686–729.
- Christensen, P.R., Ruff, S.W., Ferguson, R.L., Knudson, A.T., Anwar, S., Arvidson, R.E., Bandfield, J.L., Blaney, D.L., Budney, C., Calvin, W.M., Glotch, T.D., Golombek, M.P., Gorelick, N., Graff, T.G., Hamilton, V.E., Hayes, A., Johnson, J.R., McSween, H.Y., Mehall, G.L., Mehall, L.K., Moersch, J.E., Morris, R.V., Rogers, A.D., Smith, M.D., Squyres, S.W., Wolff, M.J., Wyatt, M.B., 2004a. Initial results from the Mini-TES experiment in Gusev Crater from the Spirit Rover. *Science* 305 (5685), 837–842.
- Christensen, P.R., Wyatt, M.B., Glotch, T.D., Rogers, A.D., Anwar, S., Arvidson, R.E., Bandfield, J.L., Blaney, D.L., Budney, C., Calvin, W.M., Faracaro, A., Ferguson, R.L., Gorelick, N., Graff, T.G., Hamilton, V.E., Hayes, A.C., Johnson, J.R., Knudson, A.T., McSween, H.Y., Mehall, G.L., Mehall, L.K., Moersch, J.E., Morris, R.V., Smith, M.D., Squyres, S.W., Ruff, S.W., Wolff, M.J., 2004b. Mineralogy at Meridiani Planum from the Mini-TES experiment on the Opportunity Rover. *Science* 306 (5702), 1733–1739.
- Clancy, R.T., Wolff, M.J., Christensen, P.R., 2003. Mars aerosol studies with the MGS TES emission phase function observations: Optical depths, particle sizes, and ice cloud types versus latitude and solar longitude. *J. Geophys. Res. Planets* 108 (E9), doi:10.1029/2003JE002058. 5098.
- Clark, B.C., 1993. Geochemical components in martian soil. *Geochim. Cosmochim. Acta* 57 (19), 4575–4581.
- Dibblee, T.W., 1958. Tertiary stratigraphic units of western Mojave Desert, California. *Am. Assoc. Petr. Geol. Bull.* 42, 135–144.
- Dibblee, T.W., 1967. Areal Geology of the Western Mojave Desert California. United States Government Printing Office, Washington, DC.
- Erard, S., Calvin, W., 1997. New composite spectra of Mars, 0.4–5.7 μm. *Icarus* 130 (2), 449–460.
- Evans, D.L., Adams, J.B., 1979. Comparison of Viking Lander multispectral images and laboratory reflectance spectra of terrestrial samples. *Lunar Planet. Sci. X*, 1829–1834.
- Foley, C.N., Economou, T.E., Clayton, R.N., Dietrich, W., 2003. Calibration of the Mars Pathfinder alpha proton X-ray spectrometer. *J. Geophys. Res. Planets* 108 (E12), doi:10.1029/2002JE002018. 8095.
- Garrett, D.E., 1998. Borates: Handbook of Deposits, Processing, Properties, and Use. Academic Press, New York.
- Gellert, R., Rieder, R., Anderson, R.C., Bruckner, J., Clark, B.C., Dreibus, G., Economou, T., Klingelhoefer, G., Lugmair, G.W., Ming, D.W., Squyres, S.W., d'Uston, C., Wanke, H., Yen, A., Zipfel, J., 2004. Chemistry of rocks and soils in Gusev Crater from the alpha particle X-ray spectrometer. *Science* 305 (5685), 829–832.
- Goetz, W., Bertelsen, P., Binai, C.S., Gunnlaugsson, H.P., Hvistendahl, S.F., Kinch, K.M., Madsen, D.E., Madsen, M.B., Olsen, M., Gellert, R., Klingelhoefer, G., Ming, D.W., Morris, R.V., Rieder, R., Rodionov, D.S., de Souza, P.A., Schroder, C., Squyres, S.W., Wdowiak, T., Yen, A., 2005. Indication of drier periods on Mars from the chemistry and mineralogy of atmospheric dust. *Nature* 436 (7047), 62–65.
- Golombek, M.P., Brown, L.L., 1988. Clockwise rotation of the western Mojave Desert. *Geology* 16 (2), 126–130.
- Greeley, R., Squyres, S.W., Arvidson, R.E., Bartlett, P., Bell, J.F., Blaney, D., Cabrol, N.A., Farmer, J., Farrand, B., Golombek, M.P., Gorevan, S.P., Grant, J.A., Haldemann, A.F.C., Herkenhoff, K.E., Johnson, J., Landis, G., Madsen, M.B., McLennan, S.M., Moersch, J., Rice, J.W., Richter, L., Ruff, S., Sullivan, R.J., Thompson, S.D., Wang, A., Weitz, C.M., Whelley, P., 2004. Wind-related processes detected by the Spirit Rover at Gusev Crater, Mars. *Science* 305 (5685), 810–821.
- Haskin, L.A., Wang, A., Jolliff, B.L., McSween, H.Y., Clark, B.C., Des Marais, D.J., McLennan, S.M., Tosca, N.J., Hurovitz, J.A., Farmer, J.D., Yen, A., Squyres, S.W., Arvidson, R.E., Klingelhoefer, G., Schroder, C., de Souza, P.A., Ming, D.W., Gellert, R., Zipfel, J., Bruckner, J., Bell, J.F., Herkenhoff, K., Christensen, P.R., Ruff, S., Blaney, D., Gorevan, S., Cabrol, N.A., Crumpler, L., Grant, J., Soderblom, L., 2005. Water alteration of rocks and soils on Mars at the Spirit Rover site in Gusev Crater. *Nature* 436 (7047), 66–69.
- Herkenhoff, K.E., Squyres, S.W., Arvidson, R., Bass, D.S., Bell, J.F., Bertelsen, P., Cabrol, N.A., Gaddis, L., Hayes, A.G., Hvistendahl, S.F., Johnson, J.R., Kinch, K.M., Madsen, M.B., Maki, J.N., McLennan, S.M., McSween, H.Y., Rice, J.W., Sims, M., Smith, P.H., Soderblom, L.A., Spanovich, N., Sullivan, R., Wang, A., 2004a. Textures of the soils and rocks at Gusev Crater from Spirit's Microscopic Imager. *Science* 305 (5685), 824–826.
- Herkenhoff, K.E., Squyres, S.W., Arvidson, R., Bass, D.S., Bell, J.F., Bertelsen, P., Ehlmann, B.L., Farrand, B., Gaddis, L., Greeley, R., Grotzinger, J., Hayes, A.G., Hvistendahl, S.F., Johnson, J.R., Jolliff, B., Kinch, K.M., Knoll, A.H., Madsen, M.B., Maki, J.N., McLennan, S.M., McSween, H.Y., Ming, D.W., Rice, J.W., Richter, L., Sims, M., Smith, P.H., Soderblom, L.A., Spanovich, N., Sullivan, R., Thompson, S., Wdowiak, T., Weitz, C., Whelley, P., 2004b. Evidence from Opportunity's microscopic imager for water on Meridiani Planum. *Science* 306 (5702), 1727–1730.
- Housley, R., 2004. Nice datolite and natrolite found in the Saddleback Basalt at Boron. *Bull. Mineral. Soc. Southern California* 74 (9), 2–6.
- Klingelhoefer, G., Morris, R.V., Bernhardt, B., Schroder, C., Rodionov, D.S., de Souza, P.A., Yen, A., Gellert, R., Evlanov, E.N., Zubkov, B., Foh, J., Bonnes, U., Kankeleit, E., Gutlich, P., Ming, D.W., Renz, F., Squyres, S.W., Arvidson, R.E., 2004. Chemistry of rocks and soils at Meridiani Planum from the alpha particle X-ray spectrometer. *Science* 306 (5702), 1746–1749.
- Scott, E.R.D., Krot, A.N., Yamaguchi, A., 1997. Formation of carbonates in martian meteorite Allan Hills 84001 from shock melts. *Meteorit. Planet. Sci.* 32 (4), A117–A118.
- E., Gutlich, P., Ming, D.W., Renz, F., Wdowiak, T., Squyres, S.W., Arvidson, R.E., 2004. Jarosite and hematite at Meridiani Planum from Opportunity's Mossbauer spectrometer. *Science* 306 (5702), 1740–1745.
- Lemmon, M.T., Wolff, M.J., Smith, M.D., Clancy, R.T., Banfield, D., Landis, G.A., Ghosh, A., Smith, P.H., Spanovich, N., Whitney, B., Whelley, P., Greeley, R., Thompson, S., Bell, J.F., Squyres, S.W., 2004. Atmospheric imaging results from the Mars exploration rovers: Spirit and Opportunity. *Science* 306 (5702), 1753–1756.
- Lepper, K., McKeever, S.W.S., 2000. Characterization of fundamental luminescence properties of the Mars soil simulant JSC Mars-1 and their relevance to absolute dating of martian eolian sediments. *Icarus* 144 (2), 295–301.
- Madsen, M.B., Hvistendahl, S.F., Gunnlaugsson, H.P., Knudsen, J.M., Goetz, W., Pedersen, C.T., Dinesen, A.R., Mogensen, C.T., Olsen, M., Hargraves, R.B., 1999. The magnetic properties experiments on Mars Pathfinder. *J. Geophys. Res. Planets* 104 (E4), 8761–8779.
- Madsen, M.B., Bertelsen, P., Goetz, W., Binai, C.S., Olsen, M., Folkmann, F., Gunnlaugsson, H.P., Kinch, K.M., Knudsen, J.M., Merrison, J., Nornberg, P., Squyres, S.W., Yen, A.S., Rademacher, J.D., Gorevan, S., Myrick, T., Bartlett, P., 2003. Magnetic properties experiments on the Mars Exploration Rover Mission. *J. Geophys. Res. Planets* 108 (E12), doi:10.1029/2002JE002029. 8069.
- McSween, H.Y., Arvidson, R.E., Bell, J.F., Blaney, D., Cabrol, N.A., Christensen, P.R., Clark, B.C., Crisp, J.A., Crumpler, L.S., Des Marais, D.J., Farmer, J.D., Gellert, R., Ghosh, A., Gorevan, S., Graff, T., Grant, J., Haskin, L.A., Herkenhoff, K.E., Johnson, J.R., Jolliff, B.L., Klingelhoefer, G., Knudson, A.T., McLennan, S., Milam, K.A., Moersch, J.E., Morris, R.V., Rieder, R., Ruff, S.W., de Souza, P.A., Squyres, S.W., Wanke, H., Wang, A., Wyatt, M.B., Yen, A., Zipfel, J., 2004. Basaltic rocks analyzed by the Spirit Rover in Gusev Crater. *Science* 305 (5685), 842–845.
- Moore, H.J., Jakosky, B.M., 1989. Viking landing sites, remote-sensing observations, and physical-properties of martian surface materials. *Icarus* 81 (1), 164–184.
- Moore, D.M., Reynolds, R.C., 1997. X-Ray Diffraction and the Identification and Analysis of Clay Minerals. Oxford University Press, Oxford.
- Moore, H.J., Bickler, D.B., Crisp, J.A., Eisen, H.J., Gensler, J.A., Haldemann, A.F.C., Matijevic, J.R., Reid, L.K., Pavlacs, F., 1999. Soil-like deposits observed by Sojourner, the Pathfinder Rover. *J. Geophys. Res. Planets* 104 (E4), 8729–8746.
- Morris, R.V., Golden, D.C., Bell, J.F., Lauer, H.V., Adams, J.B., 1993. Pigmenting agents in martian soils—Inferences from spectral, Mossbauer, and magnetic-properties of nanophasic and other iron-oxides in Hawaiian Palagonitic Soil Pn-9. *Geochim. Cosmochim. Acta* 57 (19), 4597–4609.
- Morris, R.V., Golden, D.C., Bell, J.F., Shetler, T.D., Scheinost, A.C., Hinman, N.W., Furriss, G., Mertzman, S.A., Bishop, J.L., Ming, D.W., Allen, C.C., Britt, D.T., 2000. Mineralogy, composition, and alteration of Mars Pathfinder rocks and soils: Evidence from multispectral, elemental, and magnetic data on terrestrial analogue, SNC meteorite, and Pathfinder samples. *J. Geophys. Res. Planets* 105 (E1), 1757–1817.
- Morris, R.V., Klingelhoefer, G., Schroder, C., Rodionov, D.S., Yen, A., Ming, D.W., de Souza, P.A., Fleischer, I., Wdowiak, T., Gellert, R., Bernhardt, B., Evlanov, E.N., Zubkov, B., Foh, J., Bonnes, U., Kankeleit, E., Gutlich, P., Renz, F., Squyres, S.W., Arvidson, R.E., 2006a. Mossbauer mineralogy of rock, soil, and dust at Gusev Crater, Mars: Spirit's journey through weakly altered olivine basalt on the plains and pervasively altered basalt in the Columbia Hills. *J. Geophys. Res. Planets* 111 (E2), doi:10.1029/2005JE002584. E02S13.
- Morris, R.V., Klingelhoefer, G., Schroder, C., Rodionov, D.S., Yen, A., Ming, D.W., de Souza, P.A., Fleischer, I., Wdowiak, T., Gellert, R., Bernhardt, B., Bonnes, U., Cohen, B.A., Evlanov, E.N., Foh, J., Gutlich, P., Kankeleit, E., McCoy, T., Mittlefehldt, D.W., Renz, F., Schmidt, M.E., Zubkov, B., Squyres, S.W., Arvidson, R.E., 2006b. Mossbauer mineralogy of rock, soil, and dust at Meridiani Planum, Mars: Opportunity's journey across sulfate-rich outcrop, basaltic sand and dust, and hematite lag deposits. *J. Geophys. Res. Planets* 111 (E12), doi:10.1029/2006JE002791. E12S15.
- Mustard, J.F., Bell, J.F., 1994. New composite reflectance spectra of Mars from 0.4 to 3.14 μm. *Geophys. Res. Lett.* 21 (5), 353–356.
- Ormond, D.R., Kral, T.A., 2006. Washing methanogenic cells with the liquid fraction from a Mars soil simulant and water mixture. *J. Microbiol. Methods* 67 (3), 603–605.
- Peters, G.H., Smith, J.A., Mungas, G.S., Bearman, G.H., Shiraishi, L.R., Beegle, L.W., 2008. RASP based sample acquisition of analogue martian permafrost samples: Implications for NASA's Phoenix Scout Mission. *Planet. Space Sci.* 56 (3–4), 303–309.
- Pollack, J.B., Colburn, D.S., Flasar, F.M., Kahn, R., Carlson, C.E., Pidek, D., 1979. Properties and effects of dust particles suspended in the martian atmosphere. *J. Geophys. Res.* 84 (NB6), 2929–2945.
- Putirka, K., Weigand, P., 1987. Miocene Volcanic Rocks of the Western Mojave Desert, California: Evidence for Magma-Mixing. In: Abstracts with Program, vol. 19. Geological Society of America.
- Rieder, R., Gellert, R., Anderson, R.C., Bruckner, J., Clark, B.C., Dreibus, G., Economou, T., Klingelhoefer, G., Lugmair, G.W., Ming, D.W., Squyres, S.W., d'Uston, C., Wanke, H., Yen, A., Zipfel, J., 2004. Chemistry of rocks and soils at Meridiani Planum from the alpha particle X-ray spectrometer. *Science* 306 (5702), 1746–1749.
- Scott, E.R.D., Krot, A.N., Yamaguchi, A., 1997. Formation of carbonates in martian meteorite Alan Hills 84001 from shock melts. *Meteorit. Planet. Sci.* 32 (4), A117–A118.

- Siefke, J.W., 1991. The Boron open pit mine at the Kramer borate deposit. In: The Diversity of Mineral and Energy Resources of Southern California. Soc. Econ. Geol. Guidebook Ser. 12, 4–15.
- Singer, R.B., 1982. Spectral evidence for the mineralogy of high-albedo soils and dust on Mars. *J. Geophys. Res.* 87 (NB12), 159–168.
- Smith, P.H., Lemmon, M., 1999. Opacity of the martian atmosphere measured by the Imager for Mars Pathfinder. *J. Geophys. Res. Planets* 104 (E4), 8975–8985.
- Smith, P.H., Bell, J.F., Bridges, N.T., Britt, D.T., Gaddis, L., Greeley, R., Keller, H.U., Herkenhoff, K.E., Jaumann, R., Johnson, J.R., Kirk, R.L., Lemmon, M., Maki, J.N., Malin, M.C., Murchie, S.L., Oberst, J., Parker, T.J., Reid, R.J., Sablotny, R., Soderblom, L.A., Stoker, C., Sullivan, R., Thomas, N., Tomasko, M.G., Ward, W., Wegryn, E., 1997a. Results from the Mars Pathfinder camera. *Science* 278 (5344), 1758–1765.
- Smith, P.H., Tomasko, M.G., Britt, D., Crowe, D.G., Reid, R., Keller, H.U., Thomas, N., Giem, F., Rueffer, P., Sullivan, R., Greeley, R., Knudsen, J.M., Madsen, M.B., Gunnlaugsson, H.P., Hviid, S.F., Goetz, W., Soderblom, L.A., Gaddis, L., Kirk, R., 1997b. The imager for Mars Pathfinder experiment. *J. Geophys. Res. Planets* 102 (E2), 4003–4025.
- Soderblom, L.A., Anderson, R.C., Arvidson, R.E., Bell, J.F., Cabrol, N.A., Calvin, W., Christensen, P.R., Clark, B.C., Economou, T., Ehlmann, B.L., Farrand, W.H., Fike, D., Gellert, R., Glotch, T.D., Golombek, M.P., Greeley, R., Grotzinger, J.P., Herkenhoff, K.E., Jerolmack, D.J., Johnson, J.R., Jolliff, B., Klingelhofer, G., Knoll, A.H., Learner, Z.A., Li, R., Malin, M.C., McLennan, S.M., McSween, H.Y., Ming, D.W., Morris, R.V., Rice, J.W., Richter, L., Rieder, R., Rodionov, D., Schroder, C., See-los, F.P., Soderblom, J.M., Squyres, S.W., Sullivan, R., Watters, W.A., Weitz, C.M., Wyatt, M.B., Yen, A., Zipfel, J., 2004. Soils of Eagle crater and Meridiani Planum at the Opportunity Rover landing site. *Science* 306 (5702), 1723–1726.
- Squyres, S.W., Arvidson, R.E., Bell, J.F., Bruckner, J., Cabrol, N.A., Calvin, W., Carr, M.H., Christensen, P.R., Clark, B.C., Crumpler, L., Des Marais, D.J., d'Uston, C., Economou, T., Farmer, J., Farrand, W., Folkner, W., Golombek, M., Gorevan, S., Grant, J.A., Greeley, R., Grotzinger, J., Haskin, L., Herkenhoff, K.E., Hviid, S., Johnson, J., Klingelhofer, G., Knoll, A., Landis, G., Lemmon, M., Li, R., Madsen, M.B., Malin, M.C., McLennan, S.M., McSween, H.Y., Ming, D.W., Moersch, J., Morris, R.V., Parker, T., Rice, J.W., Richter, L., Rieder, R., Sims, M., Smith, M., Smith, P., Soderblom, L.A., Sullivan, R., Wanke, H., Wdowiak, T., Wolff, M., Yen, A., 2004a. The Spirit Rover's Athena science investigation at Gusev Crater, Mars. *Science* 305 (5685), 794–799.
- Squyres, S.W., Arvidson, R.E., Bell, J.F., Bruckner, J., Cabrol, N.A., Calvin, W., Carr, M.H., Christensen, P.R., Clark, B.C., Crumpler, L., Des Marais, D.J., d'Uston, C., Economou, T., Farmer, J., Farrand, W., Folkner, W., Golombek, M., Gorevan, S., Grant, J.A., Greeley, R., Grotzinger, J., Haskin, L., Herkenhoff, K.E., Hviid, S., Johnson, J., Klingelhofer, G., Knoll, A.H., Landis, G., Lemmon, M., Li, R., Madsen, M.B., Malin, M.C., McLennan, S.M., McSween, H.Y., Ming, D.W., Moersch, J., Morris, R.V., Parker, T., Rice, J.W., Richter, L., Rieder, R., Sims, M., Smith, M., Smith, P., Soderblom, L.A., Sullivan, R., Wanke, H., Wdowiak, T., Wolff, M., Yen, A., 2004b. The Opportunity Rover's Athena science investigation at Meridiani Planum, Mars. *Science* 306 (5702), 1698–1703.
- Wanke, H., Bruckner, J., Dreibus, G., Rieder, R., Ryabchikov, I., 2001. Chemical composition of rocks and soils at the Pathfinder site. *Space Sci. Rev.* 96 (1–4), 317–330.
- Yen, A.S., Gellert, R., Schroder, C., Morris, R.V., Bell, J.F., Knudson, A.T., Clark, B.C., Ming, D.W., Crisp, J.A., Arvidson, R.E., Blaney, D., Bruckner, J., Christensen, P.R., DesMarais, D.J., de Souza, P.A., Economou, T.E., Ghosh, A., Hahn, B.C., Herkenhoff, K.E., Haskin, L.A., Hurowitz, J.A., Jolliff, B.L., Johnson, J.R., Klingelhofer, G., Madsen, M.B., McLennan, S.M., McSween, H.Y., Richter, L., Rieder, R., Rodionov, D., Soderblom, L., Squyres, S.W., Tosca, N.J., Wang, A., Wyatt, M., Zipfel, J., 2005. An integrated view of the chemistry and mineralogy of martian soils. *Nature* 436 (7047), 49–54.